

Photoluminescence properties of $\text{ZrO}_2:\text{Gd}^{3+}$, $\text{ZrO}_2:\text{Gd}^{3+}-\text{Dy}^{3+}$ and $\text{ZrO}_2:\text{Gd}^{3+}-\text{Yb}^{3+}$ phosphors by Pechini method

ESRA YILDIZ*

Bozok University, Department of Chemistry, 66900 Yozgat, Turkey

$\text{Zr}_{0.99}\text{Gd}_{0.01}\text{O}_2$, $\text{Zr}_{0.98}\text{Gd}_{0.01}\text{Dy}_{0.01}\text{O}_2$ and $\text{Zr}_{0.98}\text{Gd}_{0.01}\text{Yb}_{0.01}\text{O}_2$ phosphors were synthesized by Pechini method at 1200 °C for 12 h in air. The phosphors were characterized by using X-ray powder diffraction (XRD), differential thermal analysis/thermal gravimetry (DTA/TG), scanning electron microscopy (SEM) and photoluminescence spectrofluorometer (PL). X-ray powder diffraction studies showed that the phosphors were crystallized as monoclinic and tetragonal multiphases. The particle size of the phosphors after heat treatment at 1200 °C was found to be of 200 nm to 250 nm. Luminescence studies on these phosphors have been carried out on the emission and excitation, along with lifetime measurements. The results of emission analysis indicate that the phosphors are expected to find potential applications as new optical materials.

Keywords: *photoluminescence; Pechini method; Gd^{3+} ; Dy^{3+} ; Yb^{3+}*

1. Introduction

Inorganic phosphors have been extensively investigated for application in various types of flat panel display (FPD), such as plasma display panels (PDPs), thin film electroluminescence devices (TFEL), field-emission displays (FEDs), and vacuum fluorescent displays (VFDs) [1–6]. In recent years, substantial efforts have been focused on the fabrication of composites of ceramic materials and rare-earth oxides. One of the reasons for these efforts is the combination of the optical properties of rare-earth ions and the unique qualities of ceramic materials [7]. Among these ceramic materials, zirconium oxide is a potential choice due to its superior properties such as optical transparency, chemical stability, high thermal expansion coefficient, low thermal conductivity, etc. [8]. Various rare-earth ions-doped zirconia materials can achieve special optical properties and a considerable amount of work, concerning $\text{ZrO}_2:\text{Eu}$ [9], $\text{ZrO}_2:\text{Tb}$ [10], $\text{ZrO}_2:\text{Mn}$ [11], etc. has been reported. The lanthanide ions incorporated

into zirconia materials can provide special optical properties due to structural modifications, impacting the electronic structure of the host material lattice.

As already known, rare-earth ions are filled with the inner layer of 4f electron orbital and also have different energy levels owing to different arrangements of the 4f electrons. When the transition of 4f electrons occurs among different energy levels, they can produce a large number of absorption and fluorescence spectra. Thus, rare-earth ions are often doped into many light-emitting and laser materials to synthesize natural and nonstoichiometric compounds used as excellent fluorescent materials, laser materials and materials producing electric light [12–14].

In this work, the $\text{ZrO}_2:\text{Gd}^{3+}$, $\text{ZrO}_2:\text{Gd}^{3+}-\text{Dy}^{3+}$ and $\text{ZrO}_2:\text{Gd}^{3+}-\text{Yb}^{3+}$ phosphors were synthesized by Pechini method at 1200 °C. The phase of synthesized phosphors was determined using XRD and DTA/TG. The morphology of the phosphors was studied using SEM. The photoluminescence characteristics were studied using spectrofluorometer at room temperature.

*E-mail: esra.korkmaz@bozok.edu.tr

2. Experimental

$\text{ZrO}_2:\text{Gd}^{3+}$, $\text{ZrO}_2:\text{Gd}^{3+}-\text{Dy}^{3+}$ and $\text{ZrO}_2:\text{Gd}^{3+}-\text{Yb}^{3+}$ phosphors were prepared by Pechini method. ZrCl_4 , $\text{Gd}(\text{NO}_3)_3 \cdot 6\text{H}_2\text{O}$, $\text{Dy}(\text{NO}_3)_3 \cdot 5\text{H}_2\text{O}$ and $\text{Yb}(\text{NO}_3)_3 \cdot 5\text{H}_2\text{O}$ were used as reagents. The initial compositions were $\text{Zr}_{0.99}\text{Gd}_{0.01}\text{O}_2$, $\text{Zr}_{0.98}\text{Gd}_{0.01}\text{Dy}_{0.01}\text{O}_2$ and $\text{Zr}_{0.98}\text{Gd}_{0.01}\text{Yb}_{0.01}\text{O}_2$. First, the all reagents were dissolved in distilled water under stirring. All solutions containing the mentioned cations and citric acid were mixed thoroughly in stoichiometric ratio. The ratio of total metal cations (Zr + Gd + Dy and Zr + Gd + Yb) to citric acid was 1:4. At this stage, ethylene glycol (EG) was added to citric acid (CA) in a molar ratio: EG/CA = 4:1. The colorless solution was heated on a hot plate while stirring with a magnetic stirrer to obtain a viscous solution at a temperature of 80 °C. Heating and stirring was continued until the solution started solidifying, forming a gel-like porous mass. The resulting gel was dried at 120 °C for 24 h in air. The gel was heated to burn out the organic residues and calcined at 900 °C for 12 h. The obtained precursor was then finely ground in a mortar and heated at 1100 °C and 1200 °C for 12 h, respectively.

The crystal structural characteristics of the phosphors were identified by X-ray diffraction (XRD) using a Philips PANalytical, Empyrean diffractometer (45.0 kV, 40.0 mA) with $\text{CuK}\alpha$ ($\lambda = 1.5406 \text{ \AA}$) radiation. The thermal behavior of the phosphors was evaluated by thermal gravimetry (TG) and differential thermal analysis (DTA) using a PerkinElmer diamond analyzer in the temperature range of 50 °C to 1000 °C under inert N_2 atmosphere with a heating rate of 10 °C/min. The morphological and microstructural properties of the synthesized phosphors were characterized with a LEO 440 model scanning electron microscope using an accelerating voltage of 20 kV. The excitation and photoluminescence (PL) spectra were measured by Photon Technology International Quanta Master 30 model phosphorescence/fluorescence spectrofluorometer equipped with a pulsed xenon lamp.

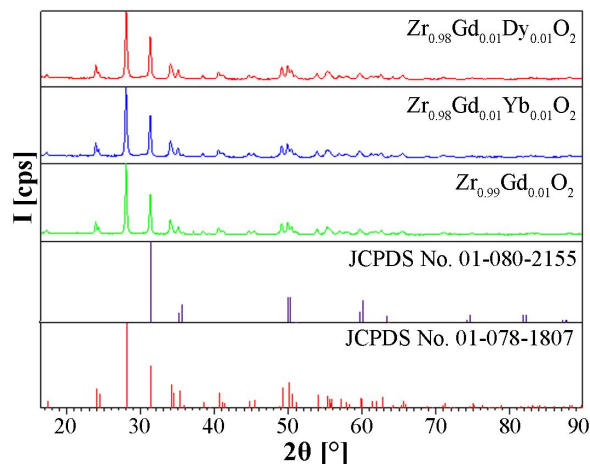


Fig. 1. X-ray diffraction patterns of $\text{Zr}_{0.99}\text{Gd}_{0.01}\text{O}_2$, $\text{Zr}_{0.98}\text{Gd}_{0.01}\text{Dy}_{0.01}\text{O}_2$ and $\text{Zr}_{0.98}\text{Gd}_{0.01}\text{Yb}_{0.01}\text{O}_2$.

3. Results and discussion

Fig. 1 shows the measured XRD powder patterns of $\text{Zr}_{0.99}\text{Gd}_{0.01}\text{O}_2$, $\text{Zr}_{0.98}\text{Gd}_{0.01}\text{Dy}_{0.01}\text{O}_2$ and $\text{Zr}_{0.98}\text{Gd}_{0.01}\text{Yb}_{0.01}\text{O}_2$ prepared at 1200 °C for 12 h in air. When the amount of rare-earth ions is 1 %, it can be found that the phosphors consist predominantly of monoclinic (m) and tetragonal (t) multiphases which were identified as the ZrO_2 monoclinic phase (JCPDS Card No. 01-078-1807) and ZrO_2 tetragonal phase (JCPDS Card No. 01-080-2155).

The DTA/TG curves of $\text{Zr}_{0.98}\text{Gd}_{0.01}\text{Yb}_{0.01}\text{O}_2$ phosphor are shown in Fig. 2. As seen in the DTA curve, no endothermic or exothermic peak is observed in the range between room temperature and 1000 °C. This observation indicates that no phase transition has occurred in the formed phosphor and it shows a high thermal stability up to around 1000 °C. This result is in agreement with the measured TG curves for which any mass change has not been detected at the heating temperature up to 1000 °C. The DTA/TG curves of the other phosphors were quite similar to the curves given in this figure.

The morphologies of the $\text{Zr}_{0.99}\text{Gd}_{0.01}\text{O}_2$, $\text{Zr}_{0.98}\text{Gd}_{0.01}\text{Dy}_{0.01}\text{O}_2$ and $\text{Zr}_{0.98}\text{Gd}_{0.01}\text{Yb}_{0.01}\text{O}_2$ phosphors after heating at 1200 °C are shown in Fig. 3. The obtained micrographs show that

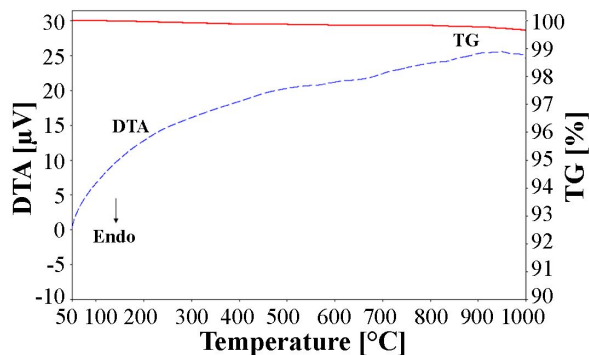


Fig. 2. DTA/TG curves of $Zr_{0.98}Gd_{0.01}Yb_{0.01}O_2$.

the particles are agglomerated and the average diameter of the grains is in the range about 200 nm to 250 nm.

The excitation and emission spectra of the $Zr_{0.99}Gd_{0.01}O_2$ phosphor are shown in Fig. 4. Two bands are observed at 275 nm and 313 nm in the excitation spectrum ($\lambda_{em} = 630$ nm). The excitation bands are related to the f-f transitions of Gd^{3+} in ZrO_2 , which corresponds to the $^8S_{7/2} \rightarrow ^6I_{11/2}$ and $^8S_{7/2} \rightarrow ^6P_{7/2}$, respectively [15]. The emission spectrum ($\lambda_{ex} = 275$ nm) shows one strong band at 635 nm due to the $^6I_{7/2} \rightarrow ^6P_{3/2}$ transition Gd^{3+} [16].

Fig. 5 shows the excitation and emission spectra of $Zr_{0.98}Gd_{0.01}Dy_{0.01}O_2$ phosphor sintered at 1200 °C for 12 h. The excitation spectrum ($\lambda_{em} = 584$ nm) has been recorded from 200 nm to 530 nm. The broad band centered at 265 nm is attributed to a charge-transfer (CT) transition, which occurs due to electron transition from the filled 2p shell of the O^{2-} to the partially filled 4f shell of Dy^{3+} [17, 18]. Totally five excitation bands are observed at 320 nm, 353 nm, 380 nm, 420 nm and 445 nm, corresponding to the $^6H_{15/2} \rightarrow ^6P_{3/2}$, $^6H_{15/2} \rightarrow ^6P_{7/2}$, $^6H_{15/2} \rightarrow ^4F_{7/2}$, $^6H_{15/2} \rightarrow ^4G_{11/2}$ and $^6H_{15/2} \rightarrow ^4I_{15/2}$ transitions of Dy^{3+} , respectively [19, 20]. There are no excitation bands of Gd^{3+} . Because there exists an overlap of energy levels of both Dy^{3+} and Gd^{3+} in the UV region, it is really difficult to differentiate more correctly in labeling the levels of Gd^{3+} ions. The emission spectrum was measured under 353 nm excitation. The emission spectrum is composed of four

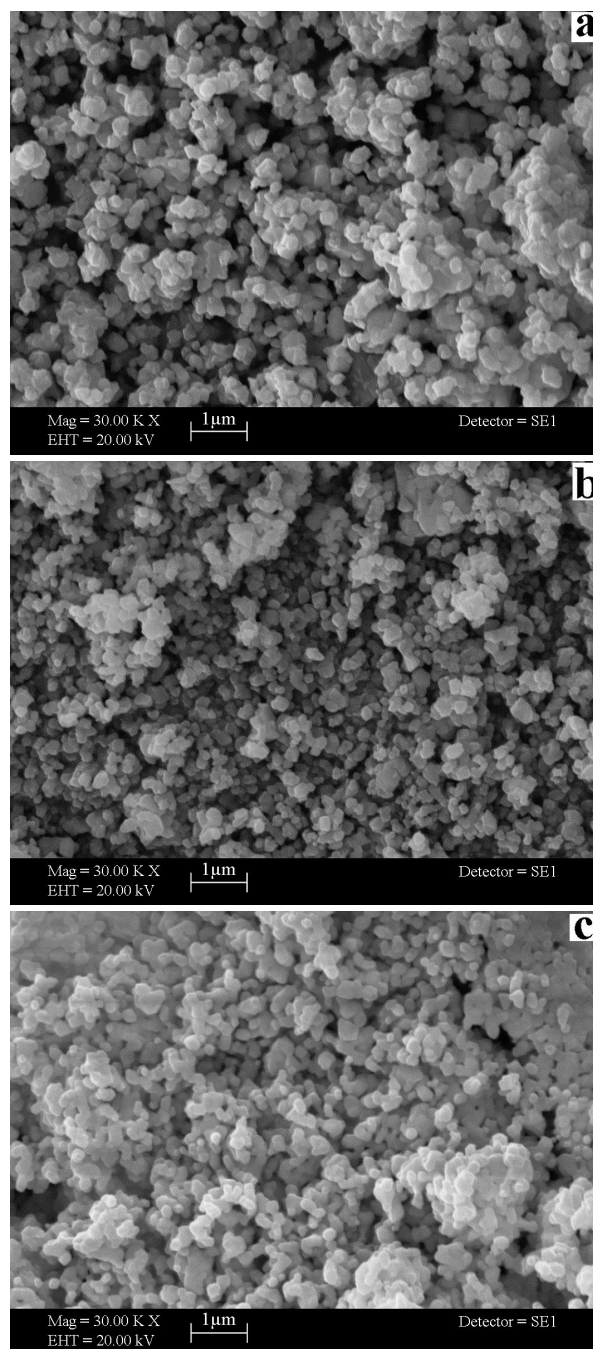


Fig. 3. The measured SEM images of (a) $Zr_{0.99}Gd_{0.01}O_2$, (b) $Zr_{0.98}Gd_{0.01}Dy_{0.01}O_2$ and (c) $Zr_{0.98}Gd_{0.01}Yb_{0.01}O_2$ phosphors.

emission peaks located at 490 nm, 586 nm, 681 nm, and 768 nm, which are ascribed to the $^4F_{9/2} \rightarrow ^6H_{15/2}$, $^4F_{9/2} \rightarrow ^6H_{13/2}$, $^4F_{9/2} \rightarrow ^6H_{11/2}$ and $^4F_{9/2} \rightarrow ^6H_{9/2}$ transitions of Dy^{3+} [21].

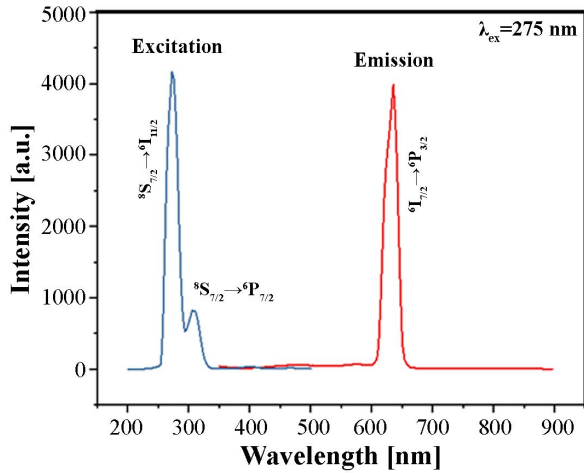


Fig. 4. Excitation and emission spectra of $\text{Zr}_{0.99}\text{Gd}_{0.01}\text{O}_2$ at room temperature.

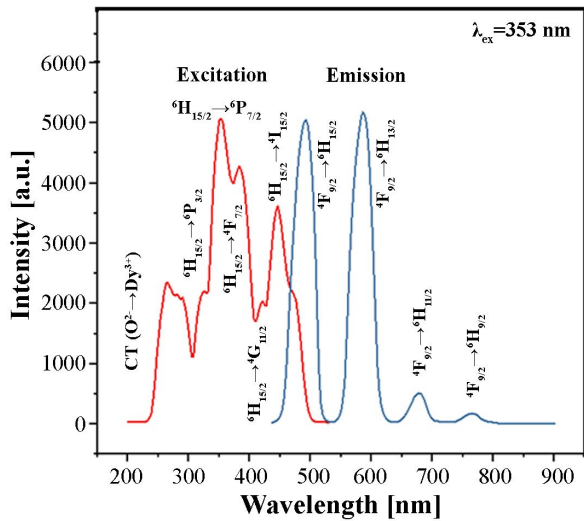


Fig. 5. Excitation and emission spectra of $\text{Zr}_{0.98}\text{Gd}_{0.01}\text{Dy}_{0.01}\text{O}_2$ at room temperature.

The excitation and emission spectra of the $\text{Zr}_{0.98}\text{Gd}_{0.01}\text{Yb}_{0.1}\text{O}_2$ phosphor are shown in Fig. 6. The excitation and emission bands are due to the transitions of Gd^{3+} ions as in Fig. 4. The electronic transitions of Yb^{3+} ions have not been observed. But Yb^{3+} co-doped $\text{ZrO}_2:\text{Gd}^{3+}$ increased the emission intensity from about 4000 a.u. to 5000 a.u. The change in the emission intensities of the doped ions can be attributed to two different reasons. The first reason is that defect centers occurring in the host crystal due to the doping of ions can increase

emission intensity. The second is that the trap centers emerging with doping can decrease the emission intensity by acting as extinction centers.

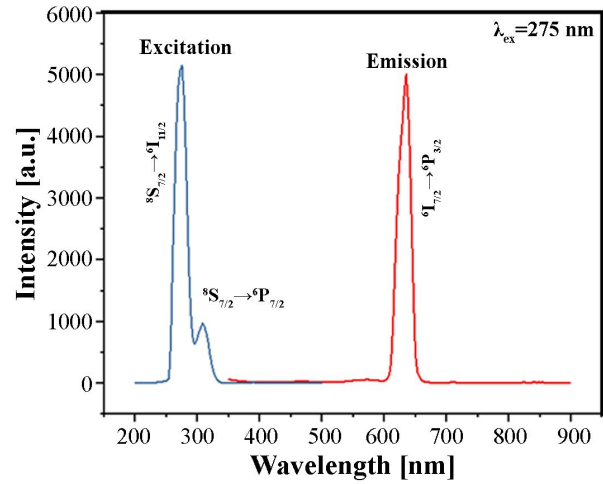


Fig. 6. Excitation and emission spectra of $\text{Zr}_{0.98}\text{Gd}_{0.01}\text{Yb}_{0.1}\text{O}_2$ at room temperature.

The decay curves of the $\text{Zr}_{0.99}\text{Gd}_{0.01}\text{O}_2$, $\text{Zr}_{0.98}\text{Gd}_{0.01}\text{Dy}_{0.01}\text{O}_2$ and $\text{Zr}_{0.98}\text{Gd}_{0.01}\text{Yb}_{0.1}\text{O}_2$ phosphors are shown in Fig. 7. Decay times can be calculated by a curve fitting procedure based on the following single exponential equation:

$$I = A_1 \exp(-t/\tau_1) + C \quad (1)$$

where I is phosphorescence intensity; A_1 and C are constants; t is time; τ_1 is lifetime for the exponential components. The decay times (τ_1) for the exponential components of the $\text{Zr}_{0.99}\text{Gd}_{0.01}\text{O}_2$, $\text{Zr}_{0.98}\text{Gd}_{0.01}\text{Dy}_{0.01}\text{O}_2$ and $\text{Zr}_{0.98}\text{Gd}_{0.01}\text{Yb}_{0.1}\text{O}_2$ phosphors are 1235 μs , 299.4 μs and 27.2 μs , respectively. The phosphor $\text{ZrO}_2:\text{Gd}^{3+}$ shows much longer afterglow than the $\text{ZrO}_2:\text{Gd}^{3+}-\text{Dy}^{3+}$ and $\text{ZrO}_2:\text{Gd}^{3+}-\text{Yb}^{3+}$ phosphors which indicates that Dy^{3+} and Yb^{3+} ions do not play an important role in prolonging the afterglow.

4. Conclusions

$\text{Zr}_{0.99}\text{Gd}_{0.01}\text{O}_2$, $\text{Zr}_{0.98}\text{Gd}_{0.01}\text{Dy}_{0.01}\text{O}_2$ and $\text{Zr}_{0.98}\text{Gd}_{0.01}\text{Yb}_{0.1}\text{O}_2$ phosphors have successfully been synthesized using Pechini method by sintering at 1200 $^\circ\text{C}$. The crystal structure, morphology, thermal properties and luminescence

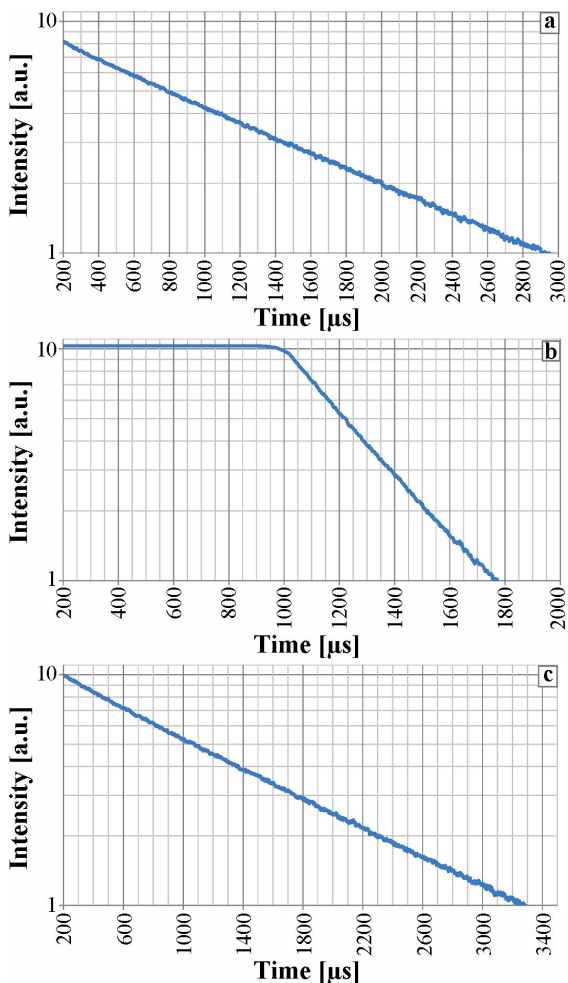


Fig. 7. The decay curves of (a) $Zr_{0.99}Gd_{0.01}O_2$, (b) $Zr_{0.98}Gd_{0.01}Dy_{0.01}O_2$ and (c) $Zr_{0.98}Gd_{0.01}Yb_{0.1}O_2$ phosphors.

properties were characterized by XRD, DTA/TG, SEM and PL, respectively. The emission spectrum of $Zr_{0.98}Gd_{0.01}Dy_{0.01}O_2$ shows two strong bands in the blue (${}^4F_{9/2} \rightarrow {}^6H_{15/2}$) and yellow (${}^4F_{9/2} \rightarrow {}^6H_{13/2}$) transitions of Dy^{3+} . The emission spectrum of $Zr_{0.99}Gd_{0.01}O_2$ shows one strong band in the red (${}^6I_{7/2} \rightarrow {}^6P_{3/2}$) transition of Gd^{3+} . The analysis of the results indicates that the $Zr_{0.99}Gd_{0.01}O_2$ and $Zr_{0.98}Gd_{0.01}Dy_{0.01}O_2$ are suitable for luminescent display device applications as well as for a white light generation.

References

- [1] HSU W.T., WU W.H., LU C.H., *Mater. Sci. Eng. B-Adv.*, 104 (2003), 40.
- [2] TSAI B.S., CHANG Y.H., CHEN Y.C., *J. Mater. Res.*, 19 (2004), 1504.
- [3] CHANG Y.S., LIN H.J., LI Y.C., CHAI Y.L., TSAI Y.Y., *J. Solid State Chem.*, 180 (2007), 3076.
- [4] MAUCH R.H., *Appl. Surf. Sci.*, 92 (1996), 589.
- [5] YI L., HOU Y., ZHAO H., HE D., XU Z., WANG Y., XU X., *Display*, 21 (2000), 147.
- [6] ZHAO X., WANG X., CHEN B., MENG Q., DI W., REN G., YANG Y., *J. Alloy. Compd.*, 433 (2007), 352.
- [7] GEDANKEN A., REISFELD R., SOMINSKI E., PAICHIK O., KOLTYPIN Y., PANCZER G., GRAFT M., MINTI H., *J. Phys. Chem. B*, 204 (2000), 7057.
- [8] HARRISON H.D.E., MCLAMED N.T., SUBBARAO E.C., *J. Electrochem. Soc.*, 110 (1963), 23.
- [9] ZHANG H.W., FU X.Y., NIU S.Y., SUN G., XIN Q., *Mater. Chem. Phys.*, 91 (2005), 361.
- [10] PIVIN J.C., GAPONENKO N.V., MOLCHAN I., KUDRAWIEC R., MISIEWICZ J., BRYJA L., THOMPSON G.E., SKELDON P., *J. Alloy. Compd.*, 341 (2002), 272.
- [11] GARCIA-HIPOLITO M., LVAREZ-FREGOSO A.O., MARTINEZ E., FALCONY C., AGUILAR-FRUITS M.A., *Opt. Mater.*, 20 (2002), 113.
- [12] XIAO X., YAN B., *Mater. Sci. Eng. B-Adv.*, 136 (2007), 154.
- [13] YADAV R.S., DUTTA R.K., KUMAR M., PANDEY A.C., *J. Lumin.*, 129 (2009), 1078.
- [14] FANG T.H., CHANG Y.S., JI L.W., PRIOR S.D., WALTER W., CHEN K.J., FANG C.N., SHEN S.T., *J. Phys. Chem. Solids*, 70 (2009), 1015.
- [15] CARNALL W.T., GOODMAN G.L., RAJNAK K., RANA R.S.A., *J. Chem. Phys.*, 90 (1989), 3443.
- [16] WEGH R.T., DONKER H., MAIJERINK A., LAMMINMAKI R.J., HOLSA J., *Phys. Rev. B*, 56 (1997), 13841.
- [17] LAI H., BAO A., YANG Y., WEIWEI X., TAO Y., YANG H., *J. Lumin.*, 128 (2008), 521.
- [18] SU X.Q., YAN B., *Mater. Chem. Phys.*, 93 (2005), 552.
- [19] LI Y.C., CHANG Y.H., LIN Y.F., CHANG Y.S., LIN Y.J., *J. Alloy. Compd.*, 439 (2007), 367.
- [20] LIU F.S., LIU Q.L., LIANG J.K., LUO J., YANG L.T., SONG G.B., ZHANG Y., WANG L.X., YAO J.N., RAO G.H., *J. Lumin.*, 111 (2005), 61.
- [21] VENKATAIAH G., JAYASANKAR C.K., *J. Mol. Struct.*, 1084 (2015), 182.

Received 2017-10-25

Accepted 2018-03-14